Original Article

Cerebral flow estimated from 3D pCASL for prediction of intraoperative blood loss in non-embolized meningiomas: a feasibility study

Xinru Deng[1,2]^, Lianjiang Lv[3], Dan Luo[1,2], Yawen Xiao[1,2], Jiankun Dai[4], Xinlan Xiao[1,2]^

[1]Department of Radiology, The Second Affiliated Hospital, Jiangxi Medical College, Nanchang University, Nanchang, China; [2]Jiangxi Provincial Key Laboratory of Intelligent Medical Imaging, Nanchang, China; [3]Department of Radiology, The First Affiliated Hospital of Nanchang University, Nanchang, China; [4]MR Research, GE Healthcare, Beijing, China

Contributions: (I) Conception and design: X Xiao, X Deng; (II) Administrative support: X Xiao, J Dai; (III) Provision of study materials or patients: L Lv, X Deng; (IV) Collection and assembly of data: X Deng, D Luo; (V) Data analysis and interpretation: X Deng, Y Xiao; (VI) Manuscript writing: All authors; (VII) Final approval of manuscript: All authors.

Correspondence to: Xinlan Xiao, MS. Department of Radiology, the Second Affiliated Hospital, Jiangxi Medical College, Nanchang University, No. 1 Minde Road, Donghu District, Nanchang 330006, China; Jiangxi Provincial Key Laboratory of Intelligent Medical Imaging, Nanchang, China. Email: jx_xiaoxinlan@sina.com.

Background: Intraoperative hemorrhage in meningioma surgery represents a critical clinical challenge. In this study, we aimed to investigate the feasibility of predicting intraoperative blood loss (IBL) in non-embolized meningiomas using the cerebral blood flow (CBF) information estimated from three-dimensional (3D) pseudo-continuous arterial spin labeling (pCASL) magnetic resonance imaging (MRI).

Methods: A total of 48 non-embolized meningioma patients who underwent preoperative 3D pCASL from September 2017 to July 2024 were retrospectively studied. IBL was recorded during the operation. The meningioma's CBF was normalized to the contralateral normal gray matter's CBF, yielding the normalized CBF, which was analyzed, along with MRI-based tumor anatomy including volume, the volume ratio between tumor and total brain (VRTB), maximum tumor diameter, and location. Patients were divided into high and low blood loss groups at a 400 mL threshold. Logistic regression was employed to find the parameters correlated with IBL. Diagnostic performance was assessed using receiver operating characteristic (ROC) curve analysis [area under the curve (AUC)] and the Delong test.

Results: Clinical and radiological analysis revealed significant differences in tumor volume, VRTB, maximum tumor diameter, and normalized CBF between subgroups. Multivariate logistic regression identified VRTB [odds ratio (OR) =2.055, 95% confidence interval (CI): 1.250–3.379], and normalized CBF (OR =1.428, 95% CI: 1.109–1.838) as significant predictors of elevated IBL. Optimal cutoff values were 3.293% for VRTB and 1.817 for normalized CBF. The AUCs were 0.751 for VRTB and 0.683 for normalized CBF, with no significant difference between them (Delong test, P=0.582). The combined risk factors' AUC, including both VRTB and normalized CBF, was 0.867, showing a significant difference from normalized CBF (P=0.010) but not from VRTB (P=0.099).

Conclusions: The normalized CBF and VRTB may serve as promising non-invasive imaging biomarkers to predict IBL and guide meningioma surgery.

Keywords: Meningioma; magnetic resonance imaging (MRI); arterial spin labeling (ASL); surgical blood loss

^ ORCID: Xinru Deng, 0009-0002-6692-1796; Xinlan Xiao, 0000-0001-9701-5062.

Submitted Oct 24, 2024. Accepted for publication Feb 26, 2025. Published online Mar 28, 2025.
doi: 10.21037/qims-24-2326
View this article at: https://dx.doi.org/10.21037/qims-24-2326

Introduction

Meningiomas represent the most prevalent tumors of the central nervous system (1). Surgical resection constitutes the principal therapeutic approach for symptomatic meningiomas, especially when complete excision is achievable (2). However, hypervascular meningiomas may lead to excessive intraoperative hemorrhage, significantly heightening the risk of adverse surgical outcomes. Although several preoperative strategies exist to mitigate this risk, such as performing embolization on hypervascular meningiomas prior to resection to minimize blood loss, the indications for these procedures remain contentious, with a lack of definitive guidelines for their implementation (3-5). Consequently, preoperative identification of hypervascular meningiomas and the predictive factors associated with intraoperative blood loss (IBL) are essential to inform and improve preoperative planning.

Digital subtraction angiography (DSA) has traditionally been utilized as a preoperative reference standard for identifying hypervascular meningiomas. Although DSA is less invasive, its potential complications include risks of sedation or anesthesia, inguinal hematoma, and ischemic stroke, indicating that it is not risk-free for patients (6,7). In addition, DSA exposes patients to ionizing radiation. Magnetic resonance imaging (MRI) is a non-invasive and ionizing radiation-free technique that has been used as the standard imaging approach for diagnosing meningioma (8). Previous studies have reported that MRI-provided anatomy information, such as tumor location and volume, are relevant factors of IBL (9-12). In addition, several studies have proposed novel indices to predict IBL, such as the tumor average T1 contrast enhancement intensity normalized to the baseline arterial value (T1 index) and the volume of flow void signal [rapid blood flow within vessels causes the area to appear as a signal loss on T2-weighted imaging (T2WI)] (10-12). However, these methods did not provide quantitative blood-related information on the tumor. A study by Kang *et al.* (13) showed that the relative cerebral blood volume and the leakage coefficient of tumor obtained from dynamic susceptibility contrast (DSC) perfusion MRI were useful markers for predicting IBL. However, DSC requires the administration of contrast agents, which may limit its application for the population for whom they are contraindicated (13).

Three-dimensional (3D) pseudo-continuous arterial spin labeling (pCASL) is a contrast agent-free MRI technique that can provide cerebral blood flow (CBF) information by using magnetic labeling of water protons in the blood, which functions as an endogenous contrast agent (14-17). 3D pCASL methodology has significant applications in the diagnosis, grading, treatment monitoring, and prognostic assessment of brain tumors (18-21), and has also been employed to predict tumor vascular distribution (22,23), offering an effective non-invasive method of clinical examination. However, it remains unknown if the CBF information obtained from 3D pCASL can be used to predict the IBL for non-embolized meningioma patients.

In this study, we aimed to investigate the value of 3D pCASL for predicting the IBL in non-embolized meningioma patients. In addition to analyzing the CBF, we also analyzed the MRI-based anatomy information of meningioma and the clinical information of patients. We present this article in accordance with the STROBE reporting checklist (available at https://qims.amegroups.com/article/view/10.21037/qims-24-2326/rc).

Methods

Patients

Patient recruitment and imaging were performed at The Second Affiliated Hospital of Nanchang University from September 2017 to July 2024. The main patient inclusion and exclusion criteria are shown in *Table 1*. None of the patients had received preoperative embolization. Clinical data were extracted including age, gender, whether there was a history of hypertension, diabetes, and coronary heart disease, pathological diagnosis and grade of meningioma, tumor consistency, and IBL. Tumor grade was based on the World Health Organization (WHO) criteria (Grades I, II, and III). IBL was recorded during surgery; IBL of 400 mL was used as the threshold to subdivide participants into low and high IBL groups (10,24). The study was conducted in accordance with the Declaration of Helsinki (as revised in 2013). This study was approved by the Ethics Committee of The Second Affiliated Hospital of Nanchang University. Given the retrospective nature of this investigation and the

Table 1 Inclusion and exclusion criteria

Project	Description
Inclusion criteria	Underwent preoperative 3D pCASL, T1-weighted imaging, T2-weighted imaging, and contrast-enhanced T1-weighted imaging
	Underwent craniotomy for tumor resection by experienced senior neurosurgeons at our institution and had a histopathological diagnosis of meningioma
	Intraoperative blood loss was recorded
Exclusion criteria	MRI images were not clear and did not meet the clinical application standards
	Received corticosteroid treatment, radiation therapy or chemotherapy, or any brain biopsy prior to the MRI

3D, three-dimensional; MRI, magnetic resonance imaging; pCASL, pseudo-continuous arterial spin labeling.

use of anonymized patient data, requirements for informed consent were waived.

MRI acquisition

Images were acquired on a 3.0 T MR scanner (Discovery 750w; GE Healthcare, Waukesha, WI, USA) with a 24-channel head and neck coil. Sponge-rubber pads were used to alleviate head motion. The full brain was covered for all the sequences used in this study. Axial T1-weighted imaging (T1WI) was scanned with repetition time (TR) of 2,007 ms, echo time (TE) of 22.6 ms, inversion time (TI) of 683.9 ms, field of view (FOV) of 258 mm × 240 mm, acquired matrix size of 320×256, reconstructed matrix size of 512×512, slice thickness of 5 mm, and slice spacing of 1.5 mm. Axial T2WI was acquired with TR of 4,841 ms, TE of 101.1 ms, FOV of 258 mm × 240 mm, acquired matrix size of 416×416, reconstructed matrix size of 512 × 512, slice thickness of 5 mm, and slice spacing of 1.5 mm. 3D pCASL scans were acquired with TR of 4,640 ms, TE of 10.7 ms, FOV of 258 mm × 240 mm, and 8 arms with 512 points per arm. All the above sequences were acquired before contrast injection. Contrast-enhanced T1-weighted (T1C) imaging was obtained after bolus injection of gadoterate meglumine (Gd-DOTA, Jiangsu Hengrui Medicine Co., Ltd., Jiangsu, China) using the identical imaging parameters of pre-contrast T1WI.

MRI data procession

Tumor location was divided into two groups: skull base and non-skull base. Maximum tumor diameter was measured on the largest area of the whole tumor. Tumor volumes were calculated from the T1C image [the region of interest (ROI) of the entire tumor was manually drawn on the T1C image using 3D-Slicer software (https://www.slicer.org/) and 3D volume of the ROI was obtained, *Figure 1A-1D*]. Whole brain volume was computed automatically using the uAIFI BrainTool (United Imaging Healthcare, Shanghai, China). The volume ratio between tumor and total brain (VRTB) was calculated. On MRI, the peritumoral edema, dural tail sign, and flow void signal were evaluated by two radiologists, and a third senior neuroradiologist would be consulted if there was no consensus reached.

3D pCASL images were transferred to a local GE post-processing workstation (AW Volume Share 4.7; GE Healthcare), then CBF maps were calculated using the embedded FuncTool software from the perfusion and the M0 calibration images within the acquired data. ROIs were placed by the radiologist blinded to the histopathology of each patient in the most densely perfused area of the meningioma at each tumor plane image (four to eight ROIs were chosen depending on tumor size, with one ROI per tumor plane, the ROI size was 45–55 mm^2), cystic, necrotic, hemorrhagic components or edema were avoided with reference to T2WI and T1C imaging. Tumor CBF was defined as the average of four to eight ROIs' CBF. To conduct the normalization, the CBF of meningioma (CBF_M) was normalized by dividing it by the CBF of contralateral normal gray matter (CBF_G) with the same size ROI, resulting in normalized CBF (nCBF) (14,25) (*Figure 1E-1G*).

Statistical analysis

Statistical analyses were performed using the software SPSS 26.0 (IBM Corp., Armonk, NY, USA), GraphPad Prism 9.0 (GraphPad Software, San Diego, CA, USA) and R statistical software (https://www.r-project.org/). For descriptive statistics, we used proportions for categorical variables, mean ± standard deviation (SD) for normal continuous data,

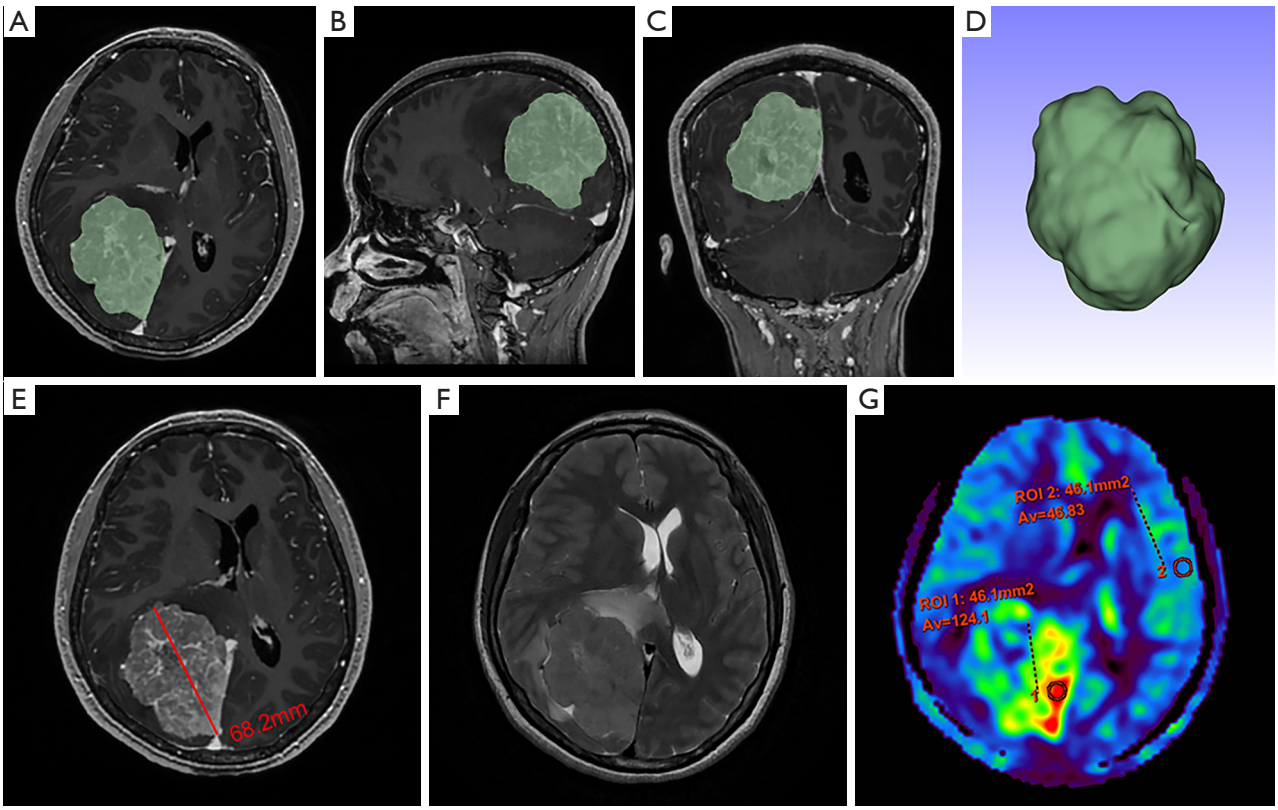

Figure 1 Delimitation of the ROI. (A-D) Final 3D volume of the ROI obtained by 3D Slicer. (E) Manual delineation of the maximum tumor diameter on the slice having the largest lesion diameter. (E-G) A cerebral blood flow map was analyzed by drawing ROIs within the most densely perfused areas of the lesion and the area of the contralateral normal gray matter with reference to T2WI and T1C imaging. 3D, three-dimensional; ROI, region of interest; T1C, T1-weighted; T2WI, T2-weighted imaging.

and median [interquartile ranges (IQR)] for non-normally continuous data. Continuous variables were compared by using the Mann-Whitney *U* test and categorical variables were compared by using the Fisher's exact test for two groups. Correlation coefficients were calculated with the Spearman test. Univariate and multivariate logistic regressions were performed to assess the predictors. The diagnostic performance of each factor to classify tumors of lower or higher IBL was assessed by using the receiver operating characteristic (ROC) curve analysis and calculation of accuracy, sensitivity, specificity, positive predictive value (PPV), and negative predictive value (NPV); the Youden index was used to assess the best cutoff value. The differences between ROC curves were assessed using the DeLong test. Differences were statistically significant when the P value was <0.05 in this study.

Results

Patient characteristics

The baseline characteristics and imaging features are summarized in *Table 2*. There were 29 women and 19 men, with a median age of 56 years. Among these 48 patients, 9 (18.75%) of the meningiomas were located at the skull base. The histology of 41 intracranial meningiomas (85.42%) was classified as WHO Grade I, and 7 (14.58%) as WHO Grade II. The median (IQR) tumor volume and VRTB were 40.81 (15.80, 57.74) cm^3 and 2.97% (1.19%, 4.33%), respectively. The median (IQR) CBF_M value and the median (IQR) nCBF value were 153.0 (80.9, 281.0) mL/100 g/min and 2.60 (1.31, 5.03) mL/100 g/min, respectively. All patients exhibited normal preoperative coagulation laboratory data.

Statistically significant differences in CBF_G were not

Table 2 Patient characteristics and inter-group dissimilarity test (Mann-Whitney *U* test or Fisher's exact test)

Parameters	Total patients (n=48)	IBL ≤400 mL (n=31)	IBL >400 mL (n=17)	P value
Age (years)	56.0 (44.3–64.0)	45.0 (56.0–64.0)	56.0 (39.5–62.5)	0.400
Gender				0.161
Male	19 (39.58)	10 (32.26)	9 (52.94)	
Female	29 (60.42)	21 (67.74)	8 (47.06)	
Tumor location				0.247
Skull base	9 (18.75)	4 (12.90)	5 (29.41)	
Non-skull base	39 (81.25)	27 (87.10)	12 (70.59)	
Hypertension	6 (12.50)	4 (12.90)	2 (11.76)	>0.99
Diabetes	3 (6.25)	2 (6.45)	1 (5.88)	>0.99
Coronary heart disease	2 (4.17)	1 (3.23)	1 (5.88)	>0.99
Tumor grade				0.226
Grade I	41 (85.42)	28 (90.32)	13 (76.47)	
Grade II	7 (14.58)	3 (9.68)	4 (23.53)	
Consistency				0.283
Soft	20 (41.67)	11 (35.48)	9 (52.94)	
Medium	19 (39.58)	14 (45.16)	5 (29.41)	
Rigid	9 (18.75)	6 (19.35)	3 (17.65)	
Peritumoral edema	39 (81.25)	25 (80.65)	14 (82.35)	>0.99
Dural tail sign	37 (77.08)	26 (83.87)	11 (64.71)	0.163
Flow void signal	17 (35.42)	8 (25.81)	9 (52.94)	0.060
Whole brain volume (cm^3)	1,388.2±146.8	1,366.5±124.5	1,427.7±178.0	0.152
Tumor volume (cm^3)	40.81 (15.80–57.74)	34.45 (9.34–47.21)	59.88 (32.36–87.25)	0.001*
VRTB (%)	2.97 (1.19–4.33)	2.36 (0.64–3.42)	4.19 (2.51–5.76)	0.004*
Maximum tumor diameter (mm)	48.06±15.05	43.61±14.87	56.18±11.91	0.008*
CBF_M (mL/100 g/min)	153.0 (80.9–281.0)	111.6 (58.6–269.5)	201.4 (124.6–524.7)	0.083
nCBF	2.60 (1.31–5.03)	1.72 (1.06–3.98)	4.43 (2.73–8.19)	0.038*
CBF_G (mL/100 g/min)	56.25 (50.31–64.16)	55.99 (51.11–67.02)	56.77 (48.08–60.84)	0.497

Data are presented as the median (interquartile range) for non-normally continuous date, mean ± standard deviation for normal continuous data, and the number (percentage) for the count data. *, P<0.05. CBF_G, the cerebral blood flow of contralateral normal gray matter; CBF_M, the cerebral blood flow of meningiomas; nCBF, normalized cerebral blood flow; IBL, intraoperative blood loss; VRTB, the volume ratio between tumor and total brain.

observed between males and females. However, significant differences were identified in CBF_M (P=0.006) and nCBF (P=0.008) between males and females (Table S1). Furthermore, there were no statistically significant differences in CBF_G, CBF_M, and nCBF across different age spans (Table S2).

Determination of variables associated with IBL

Of the total of 48 patients included in this study, the median IBL during surgery was 400 mL. IBL of 400 mL was used as the threshold to subdivide participants into low and high IBL groups (10,24). The analyses of clinical indicators

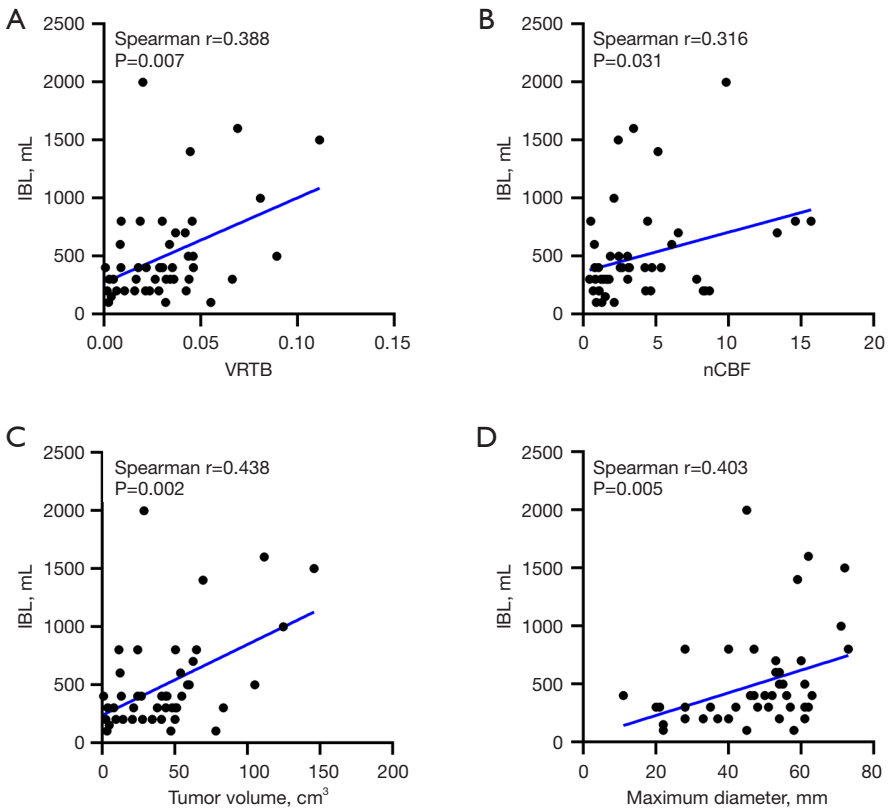

Figure 2 A scatter plot of the Spearman correlation analysis between the IBLand the VRTB (A), nCBF (B), tumor volume (C), and maximum diameter (D). IBL, intraoperative blood loss; nCBF, normalized cerebral blood flow; VRTB, the volume ratio between tumor and total brain.

showed that tumor volume, VRTB, maximum tumor diameter, and nCBF were found to be significantly different between these two subgroups. There was a moderate positive association between the IBL and tumor volume (P=0.002, r=0.438), VRTB (P=0.007, r=0.388), maximum tumor diameter (P=0.005, r=0.403), and nCBF (P=0.031, r=0.316) (*Figure 2*).

Univariate logistic regression analysis revealed that higher IBL was significantly associated with tumor volume, VRTB, maximum tumor diameter, CBF_M, and nCBF (*Figure 3*). No correlation was found between IBL and age, sex, tumor location, hypertension, diabetes, coronary heart disease, pathological grade, tumor consistency, peritumoral edema, dural tail sign, and flow void signal.

Due to the correlations between tumor volume, VRTB, and maximum tumor diameter, VRTB was ultimately selected for inclusion in the multivariate logistic regression analysis because of its highest odds ratio (OR). A high correlation was also observed between CBF_M and nCBF (r=0.963, P<0.001), leading to their separate inclusion in the multivariate logistic regression analysis. When nCBF and VRTB were included, the results indicated that VRTB [OR =2.055, 95% confidence interval (CI): 1.250–3.379] and nCBF (OR =1.428, 95% CI: 1.109–1.838) were significant predictors of IBL (*Figure 4*). Conversely, when CBF_M and VRTB were included, VRTB (OR =2.097, 95% CI: 1.255–3.503) and CBF_M (OR =1.007, 95% CI: 1.002–1.012) were also significant predictors of IBL (Table S3). However, the OR of CBF_M was lower than that of nCBF and close to one, which ultimately led to the decision to employ VRTB and nCBF in constructing the prediction model.

To assess the diagnostic efficacy of the predictors in predicting IBL, the ROC curves are shown in *Figure 5*, and the results of the ROC analysis are shown in *Table 3*. The area under the curve (AUC), best cutoff value, sensitivity, and specificity for VRTB were 0.751, 3.293%, 70.6%, and 74.2%, respectively. Those for nCBF were 0.683, 1.817, 88.2%, and 51.6%, respectively. Furthermore, the DeLong

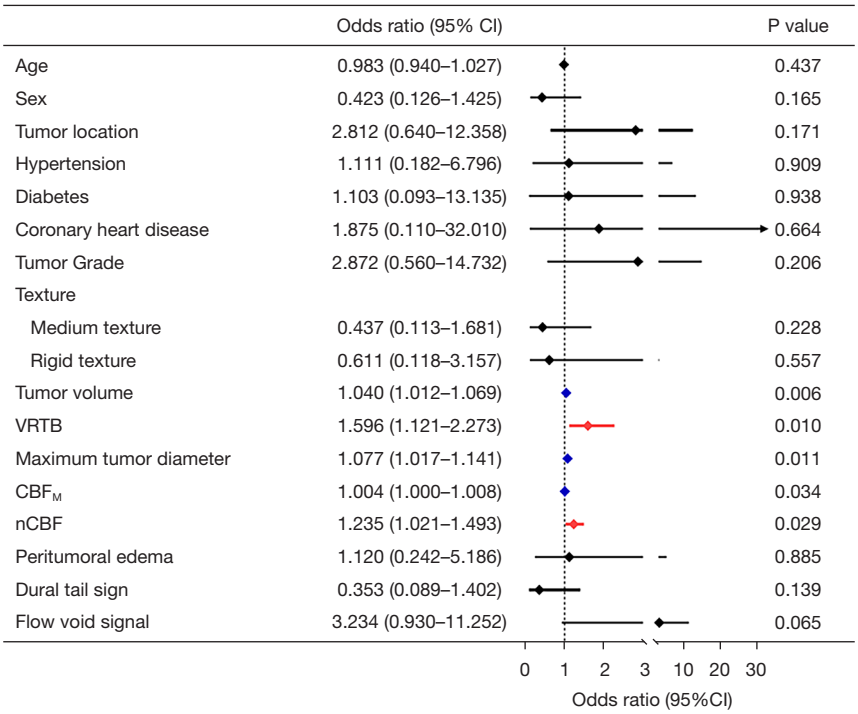

Figure 3 Univariate analysis for intraoperative blood loss. Bold represents the variables where P<0.05. CBF_M, the cerebral blood flow of meningiomas; CI, confidence interval; nCBF, normalized cerebral blood flow; VRTB, the volume ratio between tumor and total brain.

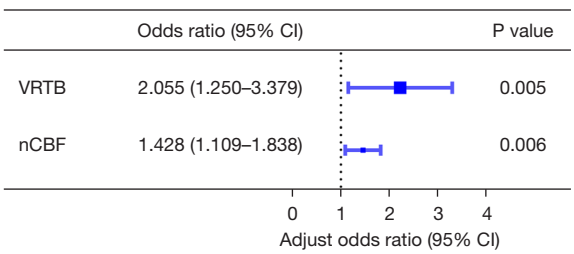

Figure 4 Stepwise multivariable logistics regression for intraoperative blood loss. CI, confidence interval; nCBF, normalized cerebral blood flow; VRTB, the volume ratio between tumor and total brain.

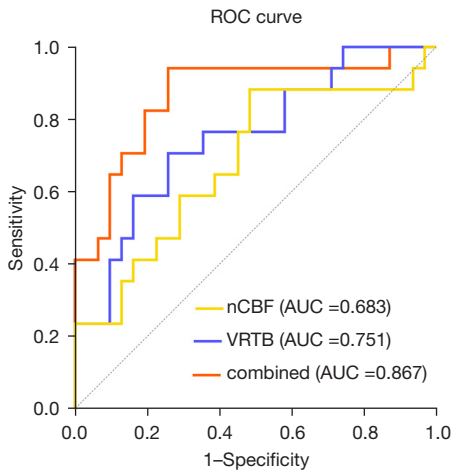

Figure 5 ROC curve for the differential diagnosis of intraoperative blood loss. AUC, area under the curve; nCBF, normalized cerebral blood flow; ROC, receiver operating characteristic; VRTB, the volume ratio between tumor and total brain.

test of the ROC curves showed no significant difference between the AUCs for VRTB and nCBF, as shown in *Table 4*.

Additionally, the AUC, sensitivity, and specificity of risk factors combined with both VRTB and nCBF were 0.867, 94.1%, and 74.2%, respectively; the differential diagnostic efficacy was improved when the two factors were combined. The DeLong test showed a significant difference between the combined and nCBF models (P=0.010), the AUC of the combined model was higher than the VRTB, although the DeLong test was not significant (P=0.099).

Discussion

Intraoperative hemorrhage in meningiomas represents a significant challenge for clinicians in terms of surgical

Table 3 Diagnostic performances of different parameters to predict intraoperative blood loss

Parameters	AUC	Cut-off score	Sensitivity (%)	Specificity (%)	Accuracy (%)	PPV (%)	NPV (%)
VRTB	0.751	3.293%	70.6	74.2	72.9	60.0	82.1
nCBF	0.683	1.817	88.2	51.6	64.6	50.0	88.9
Combined	0.867	–	94.1	74.2	81.2	66.7	95.8

AUC, area under the curve; nCBF, normalized cerebral blood flow; NPV, negative predictive value; PPV, positive predictive value; VRTB, the volume ratio between tumor and total brain.

Table 4 Comparison between receiver operating characteristic curves by DeLong's test.

Parameters	Combined-VRTB	Combined-nCBF	VRTB-nCBF
Difference between areas	0.116	0.184	0.068
Z statistic	1.648	2.586	0.551
P value	0.099	0.010	0.582

nCBF, normalized cerebral blood flow; VRTB, the volume ratio between tumor and total brain.

management (26), as increased IBL has been found to be associated with increased morbidity and mortality (27). Therefore, reduction of IBL during resection of intracranial meningiomas has been an important focus of the surgical team, such as meningioma embolization, ethmoidal artery ligation, temporary external carotid artery clamping, and intratumoral hydrogen peroxide injection. However, there is a lack of reference criteria for which patients should undergo such preoperative measures. In the present study, we obtained CBF information using 3D pCASL and employed logistic regression to analyze the relationship between IBL and the CBF_M, nCBF, anatomy information, imaging features of the meningioma, or the clinical information of patients.

Our findings revealed that higher nCBF and VRTB were significant independent predictors of higher IBL. The results were as expected: patients with larger volumes of meningioma or higher nCBF are more likely to experience a higher IBL during surgery. Furthermore, the AUC, sensitivity, and specificity were enhanced when both VRTB and nCBF were integrated. The DeLong test demonstrated that the difference in AUC between the combined model and the nCBF was significant, indicating that the diagnostic efficacy for predicting IBL was better when the two factors were combined.

Previous studies have used molecular markers such as von Willebrand factor (vWF), hypoxia-inducible factor-1 (3), and vascular endothelial growth factor (VEGF) (28) to assess meningioma vascularity. However, these markers are not routine tests for patients with meningioma and have limitations. In addition, previous studies have evaluated IBL of meningioma using imaging biomarkers, such as meningioma vascularity index (MVI), T1 index, corrected relative cerebral blood volume (rCBV), and leakage coefficient (K_2). Lagman *et al.* introduced the novel MVI, which quantifies the volume of flow void signal on T2-weighted MR images. The MVI shows a correlation with IBL both before and after controlling for tumor volume (11,12). However, some researchers have raised concerns about potential inherent inaccuracies in these results due to the possibility of intratumoral calcifications (13). A higher frequency of flow void signals was observed in the subgroup of patients with higher IBL, in comparison to the subgroup of patients with lower IBL (52.94% *vs.* 25.81%). Although the difference between the high and low IBL subgroups was not statistically different (P=0.06), it may reflect a trend consonant with the findings of this study.

Furthermore, post-contrast T1WI is commonly used for diagnosing meningiomas, where studies have found correlations between the presence of enhancement and vascularity, as well as between enhancement volume and blood loss (29,30). Nguyen *et al.* calculated the T1 index (defined as the average T1 contrast enhancement intensity across the tumor normalized to the value at the basilar artery) and found it to be an independent predictor of significant IBL (10). However, although contrast enhancement provides information about the disruption of the blood-brain barrier and vascular permeability in tumors,

it does not provide a true assessment of tumor vascularity (31,32).

Among various functional imaging techniques, perfusion MR imaging is particularly sensitive in depicting microvasculature and neovascularization in tumors, enabling quantitative assessment of tumor vascularity (15). Kang *et al.* conducted a quantitative analysis of vascular formation and permeability in meningiomas using DSC perfusion MR imaging to predict IBL. The results revealed that rCBV and K_2 were independent predictors of IBL/cm^3 (IBL per unit volume of meningioma) (13), and that higher rCBV may lead to higher intraoperative IBL. Supporting evidence from previous studies has shown that DSC-rCBV correlates with arterial spin labeling (ASL)-nCBF in tumor diagnostics (18,21). Our study indicates that meningioma patients exhibiting higher nCBF tend to have higher IBL during surgery.

3D pCASL is another perfusion imaging method that utilizes arterial blood water as an endogenous freely diffusible tracer (33). This methodology employs post-labeling delay (PLD) between the application of the labeling pulse and image acquisition in order to allow for the labeled bolus to flow into the target tissue in the imaging region. For the purpose of CBF quantification using 3D pCASL, the ideal case is that the PLD is set just longer than the longest value of arterial transit time (ATT) present in the patient. Given the ATT varies between individuals, regionally, and between healthy and pathological tissue, the optimal PLD should be different accordingly (34-36). Consequently, the selection of PLD is a compromise, such that in the majority of cases, the ASL signal will accurately reflect CBF (37). It was considered that the relatively short PLD ASL was sensitive to the early arriving cerebral blood and offered a better signal-to-noise ratio (SNR) (38). In addition, the previous study demonstrated that the degree of change in cerebral circulation is more substantial at shorter PLDs than at longer PLDs (39). Consequently, the short PLDs are regarded as being suitable for detecting minor alterations in cerebral circulation and sensitively reflect hemodynamics (39,40). The PLD of 1,525 ms was utilized in the present study cohort, which is similar to that used in a previous study on meningiomas (41).

Our study revealed that nCBF values are significantly predictive factors of increased IBL in meningioma surgery. A substantial body of evidence exists demonstrating a correlation between CBF values obtained from ASL and intracranial tumor vascularity (14,42,43); consequently, ASL is capable of identifying hypervascular tumors and quantitatively analyzing tumor perfusion (6). Furthermore, IBL is closely associated with tumor vascularity and perfusion characteristics. The current research indicated that higher CBF_M or nCBF values reflect increased tumor perfusion, which correlates with a trend towards increased IBL. A high correlation was identified between CBF_M and nCBF, consistent with the findings of previous research (20). However, the OR for nCBF was greater in predicting IBL, suggesting that nCBF is a more effective predictor, which may be due to the fact that it reduces some individual differences (14).

As in the case of *Figure 6*, both meningiomas exhibit a markedly heterogeneous enhancement on the T1C sequence. However, there is a notable discrepancy in perfusion between the two meningiomas on ASL imaging. In the case of the second patient (*Figure 6E-6H*), the meningiomas' nCBF value of 13.365 leads us to surmise that the IBL is likely to exceed 400 mL. This inference will inform the clinicians to implement a suite of perioperative blood conservation strategies, including preoperative blood preparation, intraoperative autologous blood transfusion, pharmacological interventions, and possibly preoperative vascular embolization (12,13). In fact, the IBL for this patient was 700 mL, with a pathological diagnosis of angiomatous meningioma, characterized by an abundance of small blood vessels within the tumor tissue, thus presenting a higher perfusion level. In contrast, the first patient (*Figure 6A-6C*) showed a pronounced enhancement but a subdued perfusion level, with an nCBF value of 1.282 and an IBL of 100 mL. The pathological type is classified as a transitional meningioma, featuring common whirlpool-like structures and psammoma bodies, indicative of a mixture of meningothelial and fibroblastic cells.

As indicated by the literature, it was found that gray matter regions exhibited lower CBF with age, and across all brain structures examined, CBF was noted to be higher in women compared to men (44). However, the present study did not reveal any statistically significant differences in CBF_G between different age groups and genders. This may be attributable to the limited sample size of the study or alterations in cerebral hemodynamics due to the presence of meningiomas. Furthermore, our investigation revealed that men exhibited higher CBF_M and nCBF compared to women, although this finding requires further validation. It is acknowledged that blood flow in meningiomas may be influenced by various factors, including the pathological histological type, feeding arteries, and size.

It is equally imperative to acknowledge that 3D pCASL

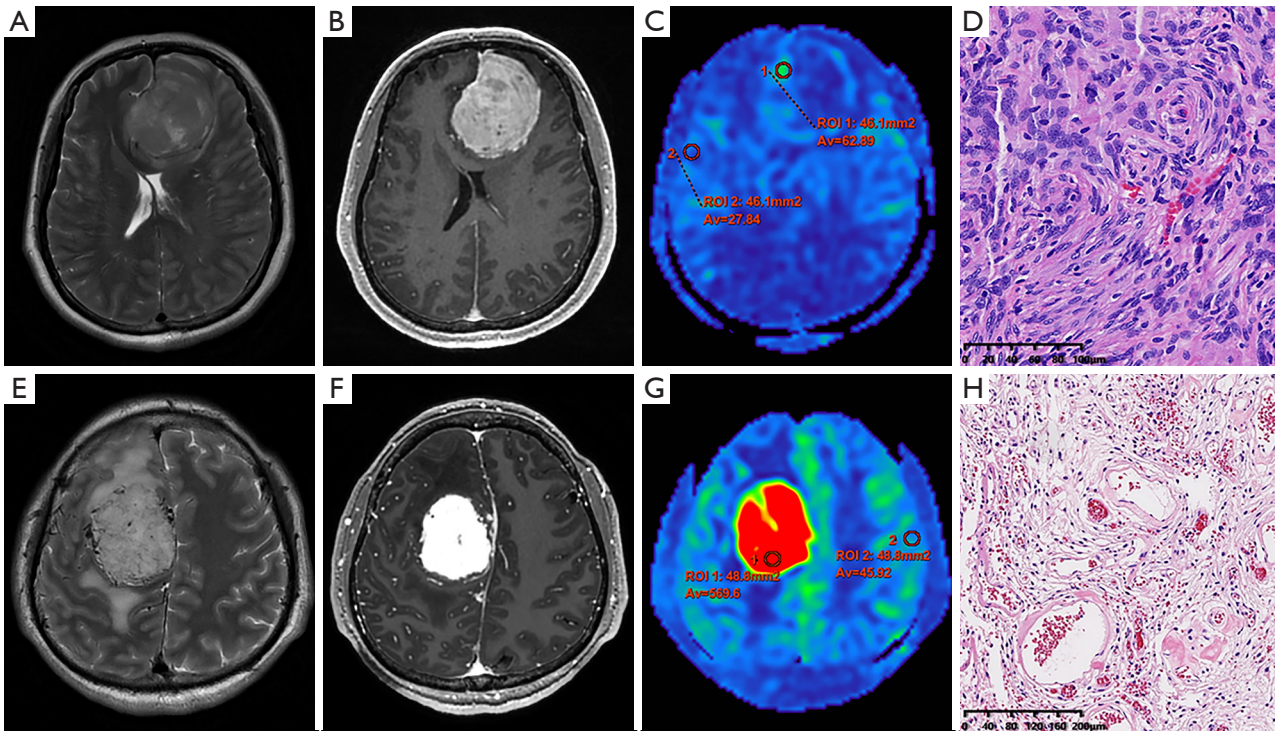

Figure 6 Representative images. (A,E) T2-weighted imaging. (B,F) Contrast-enhanced T1-weighted imaging. (C,G) Cerebral blood flow maps. (D,H) Pathological images (hematoxylin and eosin staining). (A-D) A 48-year-old female patient with transitional meningioma, the nCBF is 1.282 and the IBL is 100 mL. (E-H) A 36-year-old male patient with angiomatous meningioma, the nCBF is 13.365 and the IBL is 700 mL. nCBF, normalized cerebral blood flow; IBL, intraoperative blood loss.

stands out among a plethora of imaging techniques, demonstrating its marked superiority. An important practical advantage of 3D pCASL is its ability to avoid the need for intravenous contrast agents, making it easily repeatable and applicable to a broader range of individuals, including those with gadolinium contrast allergies, renal dysfunction, and children (45,46). Additionally, 3D pCASL offers the immediate availability and ease of quantification of perfusion images without requiring extensive post-processing (47). 3D pCASL, with its advantages of easy implementation and spatial coverage compared with single-post labeling, has emerged as a preferred labeling technique for clinical imaging, demonstrating advantages in terms of clinical feasibility (17,46). Consequently, the preoperative application of 3D pCASL represents an accessible and efficacious technique for patients afflicted with meningioma. This non-invasive modality facilitates a profound comprehension of the hemodynamic characteristics within the tumor microenvironment, clinicians are endowed with the means to discern the blood flow patterns of meningioma, thereby enhancing the precision and foresight of surgical intervention protocols.

Multiple studies to this day have revealed a significant correlation between the volumes of meningiomas and IBL (9,10,12,13); larger tumor volume is considered a factor that predicts higher IBL, mirroring the results obtained from this study. Additionally, a readily available artificial intelligence technology platform was initially utilized in this study to calculate the total intracranial volume of patients, subsequently deriving the VRTB (meningioma volume divided by total intracranial volume). In this study, both tumor volume and the VRTB were identified as independent predictive factors for IBL. However, the OR value for VRTB exceeded that of tumor volume. This finding suggests that the association between VRTB and IBL may be more substantial than that observed with tumor volume. Furthermore, the AUC value for the combined predictive factors of nCBF and VRTB was significantly higher than that of nCBF alone in predicting IBL (DeLong P value =0.010), indicating that the diagnostic efficacy for

predicting IBL is enhanced when these two factors are considered in conjunction.

The study by Lü *et al.* revealed that the origin site of meningiomas was an independent risk factor for intraoperative bleeding in 93 patients (9). However, subsequent research has presented conflicting evidence, with studies indicating that the origin site is not related to IBL (10,13). The observed discrepancy in findings may be attributed to variations in the classification of meningioma sites across different studies. In this study, we categorized the meningioma sites into the skull base group and the non-skull base group to investigate the potential correlation between meningioma location and IBL. However, the results failed to demonstrate a significant association between the meningioma location and IBL. This finding may be attributed to the limited dataset of this study, particularly the small sample size in the skull base group.

In addition, it is possible that in meningioma surgery, the IBL is more dependent on whether or not the feeding arteries can be severed early in the surgery as opposed to on the attachment site. This underscores the significant impact of the craniotomy approach on IBL during meningioma surgery. A study by Costanzo *et al.* found a significant difference in IBL when removing anterior skull base meningiomas via the pterional approach and anterior interhemispheric approach (P=0.016), with the latter showing less blood loss (48). The position of the tumor's feeding arteries determines their ease of identification and early interruption, and different craniotomy approaches affect access to these arteries (49). It is therefore hypothesized that certain approaches may offer better visualization and proximity to the tumor feeders, thus allowing for their early severance and a reduction in intraoperative bleeding.

Our study had some limitations. Firstly, it was a retrospective single-center study with a relatively small sample size, and future analyses should include a larger patient cohort. Secondly, despite the fact that all surgeries were performed by experienced senior surgeons and a standardized surgical approach of craniotomy and tumor resection was employed, there is a possibility that operator-dependent bias may have still existed. Additionally, the use of a PLD of 1,525 ms may present limitations, particularly in the elderly population. ASL with multiple PLD methods can be a good choice to handle the impact of PLD on CBF quantification, which can provide additional information on ATT and be particularly helpful in areas of arterial transit delays. Furthermore, the variation in PLDs facilitates the distinction between early macrovascular signal and genuine hyperperfusion. However, these multi-PLD methods require more time, measurements, and processing (34). Nevertheless, the selection of 1,525 ms still reflects the vascular distribution and perfusion characteristics of meningioma to some extent, and our study remains significant as we are the first to reveal the correlation between ASL and IBL during meningioma surgery.

Conclusions

Our study utilized quantitative 3D pCASL perfusion MRI in conjunction with T2WI and T1C imaging to analyze the blood flow and morphological characteristics of meningiomas. The results indicate that the VRTB and nCBF values serve as promising non-invasive imaging biomarkers to predict IBL and guide meningioma surgery, and the diagnostic efficacy for predicting IBL was better when the two factors were combined.

Acknowledgments

The authors would like to thank all the study investigators, staff, clinicians, nurses, and technicians for dedicating their time and skills to the completion of this study.

Footnote

Reporting Checklist: The authors have completed the STROBE reporting checklist. Available at https://qims.amegroups.com/article/view/10.21037/qims-24-2326/rc

Funding: None.

Conflicts of Interest: All authors have completed the ICMJE uniform disclosure form (available at https://qims.amegroups.com/article/view/10.21037/qims-24-2326/coif). J.D. is an employee of GE HealthCare. The other authors have no conflicts of interest to declare.

Ethical Statement: The authors are accountable for all aspects of the work in ensuring that questions related to the accuracy or integrity of any part of the work are appropriately investigated and resolved. The study was conducted in accordance with the Declaration of Helsinki (as revised in 2013). This study was approved by the Ethics Committee of The Second Affiliated Hospital of Nanchang University. All participants were exempt from informed

consent due to the study's retrospective nature.

References

1. Ostrom QT, Price M, Neff C, Cioffi G, Waite KA, Kruchko C, Barnholtz-Sloan JS. CBTRUS Statistical Report: Primary Brain and Other Central Nervous System Tumors Diagnosed in the United States in 2015-2019. Neuro Oncol 2022;24:v1-v95.
2. Joshi KC, Raghavan A, Muhsen B, Hsieh J, Borghei-Razavi H, Chao ST, Barnett GH, Suh JH, Neyman G, Kshettry VR, Recinos PF, Mohammadi AM, Angelov L. Fractionated Gamma Knife radiosurgery for skull base meningiomas: a single-institution experience. Neurosurg Focus 2019;46:E8.
3. Karsy M, Burnett B, Di Ieva A, Cusimano MD, Jensen RL. Microvascularization of Grade I meningiomas: effect on tumor volume, blood loss, and patient outcome. J Neurosurg 2018;128:657-66.
4. Raper DM, Starke RM, Henderson F Jr, Ding D, Simon S, Evans AJ, Jane JA Sr, Liu KC. Preoperative embolization of intracranial meningiomas: efficacy, technical considerations, and complications. AJNR Am J Neuroradiol 2014;35:1798-804.
5. James RF, Kramer DR, Page PS, Gaughen JR Jr, Martin LB, Mack WJ. Strategic and Technical Considerations for the Endovascular Embolization of Intracranial Meningiomas. Neurosurg Clin N Am 2016;27:155-66.
6. Mayercik V, Ma M, Holdsworth S, Heit J, Iv M. Arterial Spin-Labeling MRI Identifies Hypervascular Meningiomas. AJR Am J Roentgenol 2019;213:1124-8.
7. Barros G, Feroze AH, Sen R, Kelly CM, Barber J, Hallam DK, Ghodke B, Osbun JW, Kim LJ, Levitt MR. Predictors of preoperative endovascular embolization of meningiomas: subanalysis of anatomic location and arterial supply. J Neurointerv Surg 2020;12:204-8.
8. Goldbrunner R, Stavrinou P, Jenkinson MD, Sahm F, Mawrin C, Weber DC, Preusser M, Minniti G, Lund-Johansen M, Lefranc F, Houdart E, Sallabanda K, Le Rhun E, Nieuwenhuizen D, Tabatabai G, Soffietti R, Weller M. EANO guideline on the diagnosis and management of meningiomas. Neuro Oncol 2021;23:1821-34.
9. Lü J. Correlation between preoperative imaging features and intraoperative blood loss of meningioma: a new scoring system for predicting intraoperative blood loss. J Neurosurg Sci 2013;57:153-61.
10. Nguyen HS, Janich K, Doan N, Patel M, Li L, Mueller W. Extent of T1+C Intensity Is a Predictor of Blood Loss in Resection of Meningioma. World Neurosurg 2017;101:69-75.
11. Lagman C, Ong V, Nguyen T, Alkhalid Y, Sheppard JP, Romiyo P, Azzam D, Prashant GN, Jahan R, Yang I. The Meningioma Vascularity Index: a volumetric analysis of flow voids to predict intraoperative blood loss in nonembolized meningiomas. J Neurosurg 2019;130:1547-52.
12. Ghodrati F, Mekonnen M, Mahgerefteh N, Zhang AB, Pradhan A, Mozaffari K, Duong C, Yang I. Preoperative meningioma vascularity index is associated with significantly increased intraoperative blood loss and greater risk of subtotal resection. J Neurooncol 2023;161:583-91.
13. Kang Y, Wei KC, Toh CH. Can we predict intraoperative blood loss in meningioma patients? Application of dynamic susceptibility contrast-enhanced magnetic resonance imaging. J Neuroradiol 2021;48:254-8.
14. Dangouloff-Ros V, Deroulers C, Foissac F, Badoual M, Shotar E, Grévent D, Calmon R, Pagès M, Grill J, Dufour C, Blauwblomme T, Puget S, Zerah M, Sainte-Rose C, Brunelle F, Varlet P, Boddaert N. Arterial Spin Labeling to Predict Brain Tumor Grading in Children: Correlations between Histopathologic Vascular Density and Perfusion MR Imaging. Radiology 2016;281:553-66.
15. Kimura H, Takeuchi H, Koshimoto Y, Arishima H, Uematsu H, Kawamura Y, Kubota T, Itoh H. Perfusion imaging of meningioma by using continuous arterial spin-labeling: comparison with dynamic susceptibility-weighted contrast-enhanced MR images and histopathologic features. AJNR Am J Neuroradiol 2006;27:85-93.
16. Telischak NA, Detre JA, Zaharchuk G. Arterial spin labeling MRI: clinical applications in the brain. J Magn Reson Imaging 2015;41:1165-80.
17. De Simone M, Fontanella MM, Choucha A, Schaller K, Machi P, Lanzino G, Bijlenga P, Kurz FT, Lövblad KO, De Maria L. Current and Future Applications of Arterial Spin Labeling MRI in Cerebral Arteriovenous Malformations. Biomedicines 2024;12:753.
18. Bayraktar ES, Duygulu G, Çetinoğlu YK, Gelal MF,

Apaydın M, Ellidokuz H. Comparison of ASL and DSC perfusion methods in the evaluation of response to treatment in patients with a history of treatment for malignant brain tumor. BMC Med Imaging 2024;24:70.
19. Moltoni G, Romano A, Capriotti G, Campagna G, Ascolese AM, Romano A, Dellepiane F, Minniti G, Signore A, Bozzao A. ASL, DSC, DCE perfusion MRI and 18F-DOPA PET/CT in differentiating glioma recurrence from post-treatment changes. Radiol Med 2024;129:1382-93.
20. Zeng Q, Jiang B, Shi F, Ling C, Dong F, Zhang J. 3D Pseudocontinuous Arterial Spin-Labeling MR Imaging in the Preoperative Evaluation of Gliomas. AJNR Am J Neuroradiol 2017;38:1876-83.
21. Ma H, Wang Z, Xu K, Shao Z, Yang C, Xu P, Liu X, Hu C, Lu X, Rong Y. Three-dimensional arterial spin labeling imaging and dynamic susceptibility contrast perfusion-weighted imaging value in diagnosing glioma grade prior to surgery. Exp Ther Med 2017;13:2691-8.
22. Troudi A, Tensaouti F, Baudou E, Péran P, Laprie A. Arterial Spin Labeling Perfusion in Pediatric Brain Tumors: A Review of Techniques, Quality Control, and Quantification. Cancers (Basel) 2022.
23. Chatha G, Dhaliwal T, Castle-Kirszbaum MD, Amukotuwa S, Lai L, Kwan E. The utility of arterial spin labelled perfusion-weighted magnetic resonance imaging in measuring the vascularity of high grade gliomas - A prospective study. Heliyon 2023;9:e17615.
24. Wang C, Li P. Risk factors for intraoperative blood loss in resection of intracranial meningioma: Analysis of 530 cases. PLoS One 2023;18:e0291171.
25. Sunwoo L, Yun TJ, You SH, Yoo RE, Kang KM, Choi SH, Kim JH, Sohn CH, Park SW, Jung C, Park CK. Differentiation of Glioblastoma from Brain Metastasis: Qualitative and Quantitative Analysis Using Arterial Spin Labeling MR Imaging. PLoS One 2016;11:e0166662.
26. Lamszus K, Lengler U, Schmidt NO, Stavrou D, Ergün S, Westphal M. Vascular endothelial growth factor, hepatocyte growth factor/scatter factor, basic fibroblast growth factor, and placenta growth factor in human meningiomas and their relation to angiogenesis and malignancy. Neurosurgery 2000;46:938-47; discussion 947-8.
27. Zhang R, Shen Y, Bai Y, Zhang X, Wei W, Lin R, Feng Q, Wang M, Zhang M, Nittka M, Koerzdoerfer G, Wang M. Application of magnetic resonance fingerprinting to differentiate grade I transitional and fibrous meningiomas from meningothelial meningiomas. Quant Imaging Med Surg 2021;11:1447-57.
28. Hess K, Spille DC, Adeli A, Sporns PB, Zitta K, Hummitzsch L, Pfarr J, Stummer W, Brokinkel B, Berndt R, Albrecht M. Occurrence of Fibrotic Tumor Vessels in Grade I Meningiomas Is Strongly Associated with Vessel Density, Expression of VEGF, PlGF, IGFBP-3 and Tumor Recurrence. Cancers (Basel) 2020.
29. Ali R, Khan M, Chang V, Narang J, Jain R, Marin H, Rock J, Kole M. MRI Pre- and Post-Embolization Enhancement Patterns Predict Surgical Outcomes in Intracranial Meningiomas. J Neuroimaging 2016;26:130-5.
30. Catapano JS, Whiting AC, Mezher AW, Przybylowski CJ, See AP, Labib MA, Fredrickson VL, Cavalcanti DD, Lawton MT, Ducruet AF, Albuquerque FC, Sanai N. Postembolization Change in Magnetic Resonance Imaging Contrast Enhancement of Meningiomas Is a Better Predictor of Intraoperative Blood Loss Than Angiography. World Neurosurg 2020;135:e679-85.
31. Warmuth C, Gunther M, Zimmer C. Quantification of blood flow in brain tumors: comparison of arterial spin labeling and dynamic susceptibility-weighted contrast-enhanced MR imaging. Radiology 2003;228:523-32.
32. Cebeci H, Aydin O, Ozturk-Isik E, Gumus C, Inecikli F, Bekar A, Kocaeli H, Hakyemez B. Assesment of perfusion in glial tumors with arterial spin labeling; comparison with dynamic susceptibility contrast method. Eur J Radiol 2014;83:1914-9.
33. Batalov AI, Zakharova NE, Pronin IN, Belyaev AY, Pogosbekyan EL, Goryaynov SA, Bykanov AE, Tyurina AN, Shevchenko AM, Solozhentseva KD, Nikitin PV, Potapov AA. 3D pCASL-perfusion in preoperative assessment of brain gliomas in large cohort of patients. Sci Rep 2022;12:2121.
34. Alsop DC, Detre JA, Golay X, Günther M, Hendrikse J, Hernandez-Garcia L, Lu H, MacIntosh BJ, Parkes LM, Smits M, van Osch MJ, Wang DJ, Wong EC, Zaharchuk G. Recommended implementation of arterial spin-labeled perfusion MRI for clinical applications: A consensus of the ISMRM perfusion study group and the European consortium for ASL in dementia. Magn Reson Med 2015;73:102-16.
35. Yu H, Ouyang Y, Feng Y, Sun S, Zhang L, Liu Z, Tian H, Xie S. Comparison of single-postlabeling delay and seven-delay three-dimensional pseudo-continuous arterial spin labeling in the assessment of intracranial atherosclerotic disease. Quant Imaging Med Surg 2023;13:2514-25.
36. Xiao Y, Chen S, Zhang Z, Huang J, Gui Y, Luo D, Deng X, Dai J, Xiao X. Three-dimensional pseudocontinuous arterial spin labeling with dual postlabeling delay for

reflecting cerebral blood flow regulation in patients with hydrocephalus: a retrospective cross-sectional study. Quant Imaging Med Surg 2024;14:5861-76.
37. Woods JG, Achten E, Asllani I, Bolar DS, Dai W, Detre JA, et al. Recommendations for quantitative cerebral perfusion MRI using multi-timepoint arterial spin labeling: Acquisition, quantification, and clinical applications. Magn Reson Med 2024;92:469-95.
38. Lindner T, Bolar DS, Achten E, Barkhof F, Bastos-Leite AJ, Detre JA, et al. Current state and guidance on arterial spin labeling perfusion MRI in clinical neuroimaging. Magn Reson Med 2023;89:2024-47.
39. Itagaki H, Kokubo Y, Kawanami K, Sato S, Yamada Y, Sato S, Sonoda Y. Arterial spin labeling magnetic resonance imaging at short post-labeling delay reflects cerebral perfusion pressure verified by oxygen-15-positron emission tomography in cerebrovascular steno-occlusive disease. Acta Radiol 2021;62:225-33.
40. Mizowaki T, Hosoda K, Inoue S, Kuroda R, Kurihara E. Pseudo-continuous arterial spin labeling with short post-labeling delay time sensitively reflects the hemodynamics of symptomatic patients with permanent large vessel occlusion before and after revascularization. Neuroradiol J 2022;35:706-12.
41. Singh B, Agrawal D, Garg A, Singh M, Chandra PS, Kale SS. A Prospective Study on Perfusion MRI Changes in Intracranial Meningiomas Following Gamma Knife Therapy. Neurol India 2024;72:763-7.
42. Noguchi T, Yoshiura T, Hiwatashi A, Togao O, Yamashita K, Nagao E, Shono T, Mizoguchi M, Nagata S, Sasaki T, Suzuki SO, Iwaki T, Kobayashi K, Mihara F, Honda H. Perfusion imaging of brain tumors using arterial spin-labeling: correlation with histopathologic vascular density. AJNR Am J Neuroradiol 2008;29:688-93.
43. Ningning D, Haopeng P, Xuefei D, Wenna C, Yan R, Jingsong W, Chengjun Y, Zhenwei Y, Xiaoyuan F. Perfusion imaging of brain gliomas using arterial spin labeling: correlation with histopathological vascular density in MRI-guided biopsies. Neuroradiology 2017;59:51-9.
44. Alisch JSR, Khattar N, Kim RW, Cortina LE, Rejimon AC, Qian W, Ferrucci L, Resnick SM, Spencer RG, Bouhrara M. Sex and age-related differences in cerebral blood flow investigated using pseudo-continuous arterial spin labeling magnetic resonance imaging. Aging (Albany NY) 2021;13:4911-25.
45. Hirai T, Kitajima M, Nakamura H, Okuda T, Sasao A, Shigematsu Y, Utsunomiya D, Oda S, Uetani H, Morioka M, Yamashita Y. Quantitative blood flow measurements in gliomas using arterial spin-labeling at 3T: intermodality agreement and inter- and intraobserver reproducibility study. AJNR Am J Neuroradiol 2011;32:2073-9.
46. Haller S, Zaharchuk G, Thomas DL, Lovblad KO, Barkhof F, Golay X. Arterial Spin Labeling Perfusion of the Brain: Emerging Clinical Applications. Radiology 2016;281:337-56.
47. Tanaka Y, Kohno M, Hashimoto T, Nakajima N, Izawa H, Okada H, Ichimasu N, Matsushima K, Yokoyama T. Arterial spin labeling imaging correlates with the angiographic and clinical vascularity of vestibular schwannomas. Neuroradiology 2020;62:463-71.
48. Costanzo R, Scalia G, Porzio M, Benigno U, Gerardi RM, Maugeri R, Iacopino DG, Furnari M, Vasta G, Umana GE, Nicoletti GF, Graziano F. Pterional versus anterior interhemispheric approach in anterior skull base meningiomas: A comparative study. Interdiscip Neurosurg 2023;33:101766.
49. Bruneau M, George B. Foramen magnum meningiomas: detailed surgical approaches and technical aspects at Lariboisière Hospital and review of the literature. Neurosurg Rev 2008;31:19-32; discussion 32-3.

Cite this article as: Deng X, Lv L, Luo D, Xiao Y, Dai J, Xiao X. Cerebral flow estimated from 3D pCASL for prediction of intraoperative blood loss in non-embolized meningiomas: a feasibility study. Quant Imaging Med Surg 2025;15(4):3308-3321. doi: 10.21037/qims-24-2326

